

## EFFECT OF CHARGE CARRIER TRAPPING ON GERMANIUM COAXIAL DETECTOR LINE SHAPES

Thomas W. RAUDORF

*EG&G ORTEC, 100 Midland Road, Oak Ridge, TN 37830, USA*

Richard H. PEHL

*Lawrence Berkeley Laboratory, University of California, Berkeley, CA 94720, USA*

Received 28 October 1986

A theoretical method to predict and quantify the effects of charge carrier trapping on germanium coaxial detector line shapes has been developed. This model was used to calculate line shapes which closely matched the measured line shapes of both conventional and reverse electrode high-purity germanium coaxial detectors that had suffered fast neutron damage. In accordance with experimentally established behavior, the theory predicts that reverse electrode detectors are vastly more resistant to the effects of neutron damage than conventional electrode detectors. The theory also predicts that the energy resolution and line shape of neutron-damaged conventional electrode detectors are far more dependent on detector diameter than are detectors of the reverse electrode configuration. The generally observed variation of the energy resolution and line shape as a function of bias voltage is shown to arise from an  $\mathcal{E}^{-1}$  dependence of the trap cross section on electric field.

### 1. Introduction

The trapping of charge carriers and the resultant decrease in charge collection efficiency is well known to degrade the line shapes of spectral peaks produced by germanium gamma-ray spectrometers. A determination of the parameters which affect these detector line shapes would therefore be instrumental to a better understanding of the charge collection and carrier trapping processes in germanium detectors. Various attempts to calculate detector line shapes have been made, the most successful [1–3] being based on the model proposed by Trammell and Walter [1]. These earlier studies were primarily concerned with the effects of incomplete charge collection in germanium planar detectors. A new study of line shape theory with particular application to coaxial detectors would be very helpful in further characterizing the charge collection processes in high-purity germanium (HPGe) material. Germanium coaxial detectors exhibit the influence of trapping more severely than planar detectors because carrier trapping becomes a relatively more significant factor in the higher energy region where coaxial detectors are usually operated.

A good test of any model would be the degree of correspondence of the line shapes calculated from that model to the spectra obtained from neutron-damaged coaxial detectors. Damage centers caused by fast neutron irradiation are an important source of charge carrier trapping and, therefore, performance degradation in

germanium detectors. This performance degradation is more severe in coaxial detectors with the  $n^+$  contact on the outside (conventional geometry fabricated from p-type material) than in coaxial detectors with the  $p^+$  contact on the outside (reverse geometry fabricated from n-type material) [4]. Unfortunately, the actual number of controlled experimental studies on fast neutron damage of HPGe coaxial detectors is small. Even less has been done on the radiation damage resistance of conventional versus reverse geometry coaxial detectors. This certainly is not an indication of lack of concern about the subject. In fact, the opposite is true. Great interest exists in the properties of radiation-damaged HPGe coaxial detectors because these devices are commonly used in neutron radiation fields. However, since HPGe coaxial detectors are expensive and would not willingly be damaged by either a manufacturing or user group, many questions concerning radiation damage are unlikely to be resolved experimentally. A line shape theory for HPGe coaxial detectors would, therefore, be of great value if the calculated spectra could be used to predict performance degradation after exposure to a known neutron fluence.

The objectives of the present study are to develop a general theory to describe line shapes of HPGe coaxial detectors, then to apply the theory to the specific subject of fast neutron damage in these devices. True coaxial detectors having both conventional and reverse geometries with varying concentrations of uniformly

distributed hole traps will be considered; no electron trapping will be assumed. These conditions approximate the experimental situation very well. The mean free path of fast neutrons in germanium ( $\sim 6$  cm) is sufficiently long to ensure that the damage will be more or less uniformly distributed; it also has been determined that neutron-induced damage centers almost exclusively trap holes [5]. Uniform gamma-ray irradiation and true coaxial detector geometry (rather than the closed-end geometry currently favored by most manufacturers) are assumptions which approximate the experimental case fairly well and facilitate the computation of the resulting line shape.

## 2. Theory

As was done in previous studies [1-3], the Trammell-Walter relationship (eq. (1)) is taken as an appropriate starting point. Trammell and Walter considered the distribution of pulse heights resulting from gamma-ray interactions within an infinitesimal cross-sectional slice of the detector. Integration over the detector volume was shown to yield the fraction of total events having pulse heights within the energy interval  $E$  to  $E + dE$  by summing the contribution from these infinitesimal volume elements. For a true coaxial detector the Trammell-Walter equation may be written as:

$$\frac{dN(E)}{dE} = \frac{1}{\sqrt{2\pi}} \int_{r_1}^{r_2} \frac{F(r)}{\sigma(r)} \times \exp \left[ -\frac{1}{2} \left( \frac{E - \eta(r) E_0}{\sigma(r)} \right)^2 \right] dr, \quad (1)$$

where

$r_1$  is the inner detector radius,

$r_2$  is the outer detector radius,

$E_0$  is the energy of the incident gamma ray.

$dN(E)/dE$ , which experimentally is proportional to the number of counts per multichannel analyzer channel, is the rate of change with energy, at energy  $E$ , of the fraction of the total number of events occurring.  $dN(E)/dE$  hence gives a value for one point on a complete line shape curve. An entire line shape may be generated by varying  $E$  about  $E_0$  and performing multiple integrations for the different  $dN(E)/dE$  values.  $F(r)$  is the geometrical weighting factor for coaxial geometry [6] and is given by:

$$F(r) = \frac{2r}{r_2^2 - r_1^2}.$$

Appropriate expressions need to be derived for  $\eta(r)$ , the charge collection efficiency, and  $\sigma(r)$ , the standard deviation in pulse height, both of which are functions of interaction position when trapping is present, as pointed out by Trammell and Walter [1]. The assumption of

uniform gamma-ray irradiation implies that after an appropriate averaging time, the amount of charge produced per unit volume is constant throughout the detector. Because of this assumption, no further assumption as to whether the charge was generated by single or multiple interaction events is necessary for eq. (1) to be valid. In fact, multiple interaction events would actually serve to decrease the average period required to produce homogeneous charge production density in the detector.

### 2.1. Charge collection efficiency

Assume conventional geometry, i.e., positively biased  $n^+$  contact on the outside. If an interaction takes place at  $r$ , the holes created will travel towards the inner contact which is negatively biased relative to the outer contact. If trapping occurs, the number of holes,  $n$ , that are still free after traveling  $dr''$  towards the center contact satisfies the equation:

$$dn = -n \frac{dr''}{\lambda_h}, \quad (2)$$

where  $\lambda_h$  is the mean free drift length for holes. The right hand side of eq. (2) is positive since the sign of  $dr''$  is negative because the holes travel towards the inner contact.

The fraction of holes at  $r'$  which are not captured after traveling from interaction position  $r$ , where  $r' < r$ , is therefore given by:

$$\frac{n}{n_0} = \exp \left[ \int_r^{r'} \frac{1}{\lambda_h} dr'' \right], \quad (3)$$

with  $n_0$  being the initial number of holes. If  $\lambda_h$  is not dependent on  $r$ , then:

$$n = n_0 \exp \left( -\frac{r-r'}{\lambda_h} \right). \quad (4)$$

The charge induced by the travel of  $n$  holes from  $r'$  to  $r' + dr'$  is given by [7]:

$$dQ = \frac{nq_0(r')^{-1} dr'}{\ln(r_2/r_1)}, \quad (5)$$

where  $q_0$  is the unit charge  $|e|$ . Once more in this case the sign of  $dr'$  is negative.

Combining eqs. (4) and (5) we get:

$$dQ = -\frac{n_0 q_0}{\ln(r_2/r_1)} \exp \left( -\frac{r-r'}{\lambda_h} \right) \frac{1}{r'} dr'. \quad (6)$$

The differential charge collection efficiency is  $dQ/n_0 q_0$ , hence:

$$d\eta_h(r) = \frac{dQ}{n_0 q_0} = -\frac{1}{\ln(r_2/r_1)} \exp \left( -\frac{r-r'}{\lambda_h} \right) \frac{1}{r'} dr',$$

and

$$\eta_h(r) = -\frac{1}{\ln(r_2/r_1)} \int_r^{r_1} \exp \left( -\frac{r-r'}{\lambda_h} \right) \frac{1}{r'} dr'. \quad (7)$$

This integral may be evaluated as a power series by using tables. Terms of higher power than the quadratic can be neglected when  $\lambda_h \gg r$  thus:

$$\eta_h(r) = -\frac{e^{-r/\lambda_h}}{\ln(r_2/r_1)} \left[ \ln \frac{r_1}{r} - \frac{1}{\lambda_h} (r - r_1) - \frac{1}{4\lambda_h^2} (r^2 - r_1^2) \right]. \quad (8)$$

For electrons a similar expression exists:

$$\eta_e(r) = \frac{e^{r/\lambda_e}}{\ln(r_2/r_1)} \left[ \ln \frac{r_2}{r} - \frac{1}{\lambda_e} (r_2 - r) + \frac{1}{4\lambda_e^2} (r_2^2 - r^2) \right]. \quad (9)$$

The total charge collection efficiency for a coaxial detector of conventional geometry then is:

$$\eta(r) = \eta_h(r) + \eta_e(r). \quad (10)$$

If the exponentials are expanded and only linear terms considered, eq. (10) reduces to the expression derived by Trammell [8]. The charge collection efficiency for the reverse electrode geometry is calculated from eq. (10) by interchanging  $\lambda_e$  and  $\lambda_h$  in the various algebraic terms.

## 2.2. Standard deviation of pulse height distribution, $\sigma(r)$

The importance of including  $\sigma(r)$  under the integral in eq. (1) was noted by Trammell and Walter [1] and subsequently confirmed by others [2,3].

$\sigma(r)$  can be considered as consisting of three components:

$$\sigma(r) = \left[ \sigma_F^2 + \sigma_N^2 + \sigma_T^2(r) \right]^{1/2}. \quad (11)$$

$\sigma_F$  is the component of  $\sigma(r)$  due to the statistics of charge production with  $\sigma_F^2 = \epsilon FE_0$ , where  $\epsilon$  is the average energy required to create an electron-hole pair,  $F$  is the effective Fano factor and  $E_0$  is the gamma-ray energy.  $\sigma_N$  is the contribution of the electronic noise where  $\sigma_N^2 = N_{1/2}^2 / 8 \ln 2$ .  $N_{1/2}$  is the full width at half maximum (fwhm) of the electronic noise.

$\sigma_T(r)$  is the contribution to the gamma-ray peak width from trapping effects. This quantity has usually been treated empirically by fitting an expression to experimental data determined from collimated beam measurements on the particular detector under consideration. Here we propose an approach which, while still having some empirical character, does not require collimated beam measurements on the specific device for which the calculation is performed.

Guided by the development of the expression for the line width due to charge production statistics [9], we assume that the line width caused by trapping results

from a fluctuation in the number of trapped carriers,  $N_T$ . We also assume that the variance in the number of trapped carriers is proportional to the average number of trapped carriers,  $\bar{N}_T$ , or

$$\Delta^2 = \langle (N - \bar{N}_T)^2 \rangle = K \bar{N}_T, \quad (12)$$

where  $\Delta$  is the standard deviation in the number of trapped carriers and  $K$  is some constant, analogous to the Fano factor, left to be determined. Now

$$\bar{N}_T = \frac{Q_0}{q_0} [1 - \eta(r)] = \frac{E_0}{\epsilon} [1 - \eta(r)], \quad (13)$$

where  $Q_0$  is the average amount of charge created by the gamma-ray interaction. Hence:

$$\Delta = \left\{ K \frac{E_0}{\epsilon} [1 - \eta(r)] \right\}^{1/2}. \quad (14)$$

Now  $\sigma_T(r) = \epsilon \Delta$ , which converts the standard deviation into eV equivalent.

And

$$\sigma_T(r) = \left\{ \epsilon K E_0 [1 - \eta(r)] \right\}^{1/2}. \quad (15)$$

The component of the fwhm due to trapping may then be expressed as:

$$\sigma_T(r)_{\text{fwhm}} = 2.355 \left\{ \epsilon K E_0 [1 - \eta(r)] \right\}^{1/2}. \quad (16)$$

This equation is similar to the empirical expression presented by Henck et al. [10] which indicated that the trapping component of the resolution varies as  $(1 - \eta) E_0^{1/2}$ .

The task of finding a value for the constant  $K$  still remains. McMath and Martini [2] made measurements on a number of trapping Ge(Li) planar detectors. They found that, for a pulse height defect of 0.65% (i.e.,  $[1 - \eta(r)] = 0.0065$ ) due to electron trapping, the corresponding contribution to the fwhm was  $\sim 4.9$  keV at the 662 keV gamma line of  $^{137}\text{Cs}$ . When these data are put into eq. (16), a  $K$  value of  $\sim 340$  is obtained. Conversely, if this value of  $K$  is used along with the pulse height defect of 0.05% measured for hole trapping in the same device, a value of fwhm = 2.9 keV is predicted when charge production statistics and electronic noise contributions are taken into account. This is precisely the value measured by McMath and Martini, which lends support to the validity of eq. (15).

The relatively large value of  $K$  deserves some comment. The variance in the number of trapped carriers is assumed proportional to the average number of trapped carriers. However, the average number of trapped carriers is proportional to the concentration of empty traps. The fluctuation in the concentration of empty traps is probably significant in comparison to the number of carriers. The number of empty traps is linked statistically to the total trap concentration and the particular trapping and detrapping mechanisms involved, including the effect of the radioactive source

itself [11]. The constant  $K$  which reflects the variation in empty trap concentration could, therefore, have a relatively large value.

### 2.3. Functional dependence of $\lambda$

The mean free drift length,  $\lambda$ , is a convenient quantity to use in the preceding calculations. However, it remains necessary to relate it to more fundamental quantities such as the number of traps, the carrier drift velocity, the trap cross section, etc. Dividing both sides of eq. (2) by  $dt$ , we get the carrier capture rate:

$$\dot{n} = -nv_{\text{drift}}/\lambda_h, \quad (17)$$

where  $v_{\text{drift}}$  is the carrier drift velocity,  $dr''/dt$ . The capture rate of holes by trapping centers is also given by:

$$\dot{n} = -\sigma_h \langle v \rangle n n_t, \quad (18)$$

where  $\sigma_h$  is the capture cross section of the trapping centers for holes,  $\langle v \rangle$  is the thermal velocity ( $\sqrt{3kT/m^*}$  at low electric field), and  $n_t$  is the trap density. Equating the capture rates given by eqs. (17) and (18) we get:

$$\lambda_h = \frac{v_{\text{drift}}}{\sigma_h \langle v \rangle n_t}. \quad (19)$$

A similar expression may be derived for the mean free path of electrons. There is no simple analytical expression for  $v_{\text{drift}}$ . The drift velocity can, however, be approximated by the empirical expression [12]:

$$v_{\text{drift}} = \frac{\mu_0 \mathcal{E}}{[1 + (\mathcal{E}/\mathcal{E}_0)^\beta]^{1/\beta}}, \quad (20)$$

where  $\mu_0$  is the mobility at low electric field,  $\mathcal{E}$  is the electric field,  $\mathcal{E}_0$  and  $\beta$  are constants. For germanium at 80 K, values of  $\mathcal{E}_0 = 210.5$  V/cm,  $\beta = 1.36$  for holes and  $\mathcal{E}_0 = 275$  V/cm,  $\beta = 1.32$  for electrons give reasonable approximations to the experimental data [6].

There is also no simple analytical expression for the thermal velocity  $\langle v \rangle$  at the electric fields usually occurring in HPGe coaxial detectors. However, the experimental data of Pinson and Bray [13] can be used to generate an empirical expression for  $\langle v \rangle$  for holes of the form:

$$\langle v \rangle = \left\{ \frac{3.2 \times 10^{-12}}{m^*} [(a + b\mathcal{E}) - c \exp(-\mathcal{E}d)] \right\}^{1/2} \text{ cm/s}, \quad (21)$$

where  $m^*$  is the effective mass (g) and  $a = 1.5 \times 10^{-2}$  eV,  $b = 6.47 \times 10^{-6}$  eV cm/V,  $c = 5.0 \times 10^{-3}$  eV,  $d = 6.0 \times 10^{-3}$  cm/V. A similar empirical expression for electrons cannot be easily found since few experimental data are available. However, it would probably be acceptable to use eq. (21) as it stands. Eq. (19) can now be evaluated using the above expressions. An interesting

point to note is that, with increasing electric field, the drift velocity saturates and becomes constant while  $\langle v \rangle$  continues to increase slowly. This implies that  $v_{\text{drift}}/\langle v \rangle$  goes through a broad maximum and then starts to decrease slowly. This effect occurs at higher electric fields than those usually occurring in coaxial detectors. The electric field,  $\mathcal{E}$ , varies as a function of  $r$  where  $r_1 \leq r \leq r_2$ . For true coaxial geometry the  $r$  dependence of  $E$  is given by:

$$\mathcal{E} = \frac{1}{2} \frac{\rho}{\epsilon_k} r - \frac{V + \frac{1}{4}(\rho/\epsilon_k)(r_2^2 - r_1^2)}{r \ln(r_2/r_1)}, \quad (22)$$

where  $\rho$  is the charge density in the HPGe detector,  $\epsilon_k$  is the dielectric constant of germanium and  $V$  is the applied bias ( $V \geq V_D$ , where  $V_D$  is the depletion voltage).

The hole trap cross section,  $\sigma_h$ , can be estimated from the work of Darken et al. [14] for the specific case of fast neutron damage. It is reasonable to assume that  $\sigma_h$  has electric field dependence. Sher [3] quotes theoretical studies which indicate that the carrier lifetime,  $\tau$ , which is closely related to  $\sigma_h$ , varies as  $\mathcal{E}^\alpha$  where  $0.5 \leq \alpha \leq 1.0$ . Darken et al. [15] predict a variation of  $\sigma_h \propto \mathcal{E}^{-1}$  for fast neutron created disordered regions. Thus an expression of the form:

$$\sigma_h = \frac{\sigma_0}{\mathcal{E}^x} \quad 0.5 \leq x \leq 1.0 \quad (23)$$

might be used in eq. (19) with  $\sigma_0$  and  $x$  considered fitting parameters ( $\mathcal{E} \neq 0$ ).

The quantities  $v_{\text{drift}}$ ,  $\langle v \rangle$  and  $\sigma_h$  are functions of the radial position,  $r$ , since the electric field has  $r$  dependence. Hence it follows that  $\lambda_h$  is also a function of  $r$ . The hole trap density,  $n_t$ , is considered uniform throughout the coaxial detector. This is a good assumption for the case of fast neutron damage. However, if a trap of different origin with a radial or other distribution gradient were being investigated,  $n_t$  could be considered a function of  $r$  and an appropriate expression for  $n_t$  substituted into eq. (19).

For neutron damage an estimate of  $n_t$  can be made from neutron cross section data. On the other hand,  $n_t$  could also be treated as a fitting parameter of the calculation if some independent data for  $\sigma_h$  were available.

If  $\lambda_h$  is considered to be a function of  $r$ , as discussed above, then (3) must be substituted directly into eq. (6) instead of eq. (4). Eq. (7) for holes and conventional geometry then becomes:

$$\eta_h(r) = -\frac{1}{\ln(r_2/r_1)} \int_r^{r_1} \exp \left[ \int_r^{r'} \frac{1}{\lambda_h(r'')} dr'' \right] \frac{1}{r'} dr', \quad (24)$$

and must be either approximated or evaluated numerically. Similar expressions exist for electrons and for the case of reverse geometry.

Points on the line shape curve may now be calculated by solving eq. (1) using eq. (10) for  $\eta(r)$  and eq. (11) for  $\sigma(r)$ . As a first approximation, a constant value of  $\lambda_h$  or  $\lambda_e$  may be assumed otherwise eqs. (19)–(23) must be used to determine  $\lambda_h$  or  $\lambda_e$ . In the latter case, eq. (10) is given by the sum of terms similar to eq. (24). The entire line shape curve can then be determined by solving eq. (1) at various energies,  $E$ , around the incident gamma-ray energy,  $E_0$ .

### 3. Results and discussion

Line shapes simulating the effects of neutron damage were calculated from eq. (1) using a Hewlett-Packard HP85 computer to perform the required numerical integration and a plotter controlled by the HP85 to draw the spectra. Since neutron damage results in the almost exclusive trapping of holes, for computational purposes,  $\lambda_e$  was set to  $10^7$  cm, effectively ignoring electron trapping. Fig. 1 shows representative curves calculated from eq. (1).  $\lambda_h$  was held constant with respect to  $r$  and treated as a parameter of the calculation, its values being arbitrarily assumed so that the calculated energy resolutions (fwhm) would be close to the resolutions of actually measured spectra. Points from the measured spectra are included in fig. 1 for comparison with the calculation. Figs. 1a–c show a very close correspondence of the measured spectra to the line shape calculation. When the heights of the two peaks were normalized to each other, the calculation correctly predicted the rest of the line shape and the pulse height defect.

A constant value of  $\lambda_h$  with respect to  $r$  is a good approximation in many cases even though  $\lambda_h$  is a function of electric field. For the range of electric fields occurring in most coaxial detectors at their operating biases, the quantity  $v_{diff}/\langle v \rangle$  varies very slowly having an average value of  $\sim 0.45$ . The electric field dependence of  $\lambda_h$  is therefore essentially given by the field dependence of the trap cross section,  $\sigma_h$ . At a given constant bias value, the fields that ordinarily occur in coaxial detectors do not vary by orders of magnitude from one contact to the other; a factor of 2 or 3 is more usual. For a constant  $\lambda_h$  to be a useful approximation, it is only necessary that some *average value* of  $\lambda_h$  describing the situation throughout the coaxial detector exist. The good correspondence between theory and measured values, as illustrated by fig. 1, shows that this condition is fulfilled in this instance.

#### 3.1. Energy resolution dependence on fast neutron fluence

In a 1978 experiment, Pehl et al. [4] measured the effect of fast neutrons on two coaxial HPGe detectors of approximately equal relative efficiency (7%) that were fabricated from the same HPGe crystal. One de-

vice had conventional geometry while the other was of the reverse electrode configuration. They were both exposed to the same fast neutron fluence from an unmoderated  $^{252}\text{Cf}$  source (average neutron energy  $\sim 1.5$  MeV), the energy resolution of 1332 keV gamma rays being measured after each irradiation. In the present work, spectra have been calculated using a range of  $\lambda_h$  values for detectors having the same parameters as the two reported in ref. [4]. Curves of fwhm versus  $\lambda_h^{-1}$  were then generated because it was expected from eq. (19) that  $\lambda_h$  would vary inversely with the neutron fluence; however, the actual constant of proportionality was not known. For this reason, one point on each calculated curve was arbitrarily matched with one point on each experimental curve for best fit in order to compare the curves. A close correlation was found to exist between the shape of the calculated curves and the shape of the measured curves, as shown in fig. 2. In fact, fig. 2 may be used to infer an empirical relationship between  $\lambda_h$  and the neutron fluence. For these two detectors, the relationship is  $\lambda_h \approx 2.5 \times 10^{11}/n_f$  cm, where  $n_f$  is the neutron fluence. This correlation of the theory to experimental data provides a powerful tool for calculating the performance of a coaxial detector after exposure to a known fast neutron fluence. Conversely, by measuring the spectrum of a damaged device, the neutron fluence may be estimated on the basis of such line shape calculations if the energy of the neutrons is known.

#### 3.2. Line shape dependence on detector radius

Detectors with larger diameters would be expected to exhibit the effects of hole trapping more severely than devices having smaller diameters. In fact, if the expression for the charge collection efficiency of holes is examined, it may be seen that  $\eta_h(r)$  decreases as  $r_2$  increases for both conventional and reverse geometry detectors. The actual effect of the variation of radius on the line shape may be determined by varying  $r_2$ . Fig. 3 gives an example of the results of such a series of line shape calculations for (a) conventional and (b) reverse geometry HPGe coaxial detectors. The outer radius was varied between 1.3 and 4.1 cm; the values of the other variables are given in the figure caption. Fig. 4 presents the variation of the fwhm determined from calculated line shapes as a function of outer radius for both detector geometries over a range of  $\lambda_h$ .

From figs. 3a and 4a it is evident that conventional geometry coaxial detectors exhibit a striking dependence of line shape and fwhm on  $r_2$ , especially at smaller  $\lambda_h$  values. Fig. 4a also shows that the  $\lambda_h$  dependence of the calculated fwhm at a given  $r_2$  increases significantly as the radius increases. On the other hand, figs. 3b and 4b demonstrate that for a given  $\lambda_h$  the variation of the line shape and fwhm with outer radius is much less

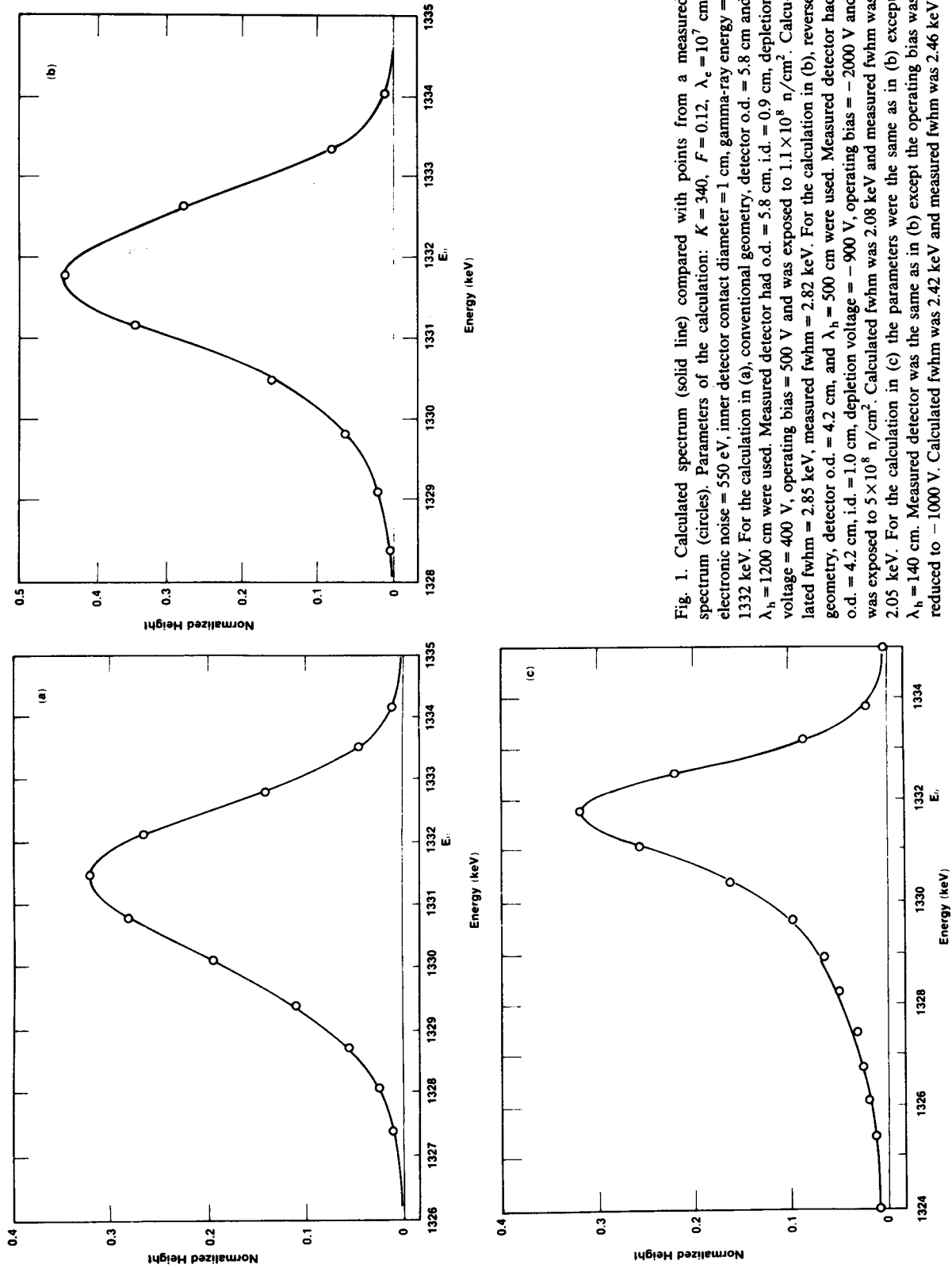


Fig. 1. Calculated spectrum (solid line) compared with points from a measured spectrum (circles). Parameters of the calculation:  $K = 340$ ,  $F = 0.12$ ,  $\lambda_c = 10^7$  cm, electronic noise = 550 eV, inner detector contact diameter = 1 cm, gamma-ray energy = 1332 keV. For the calculation in (a), conventional geometry, detector o.d. = 5.8 cm and  $\lambda_h = 1200$  cm were used. Measured detector had o.d. = 5.8 cm, i.d. = 0.9 cm, depletion voltage = 400 V, operating bias = 500 V and was exposed to  $1.1 \times 10^8$  n/cm<sup>2</sup>. Calculated fwhm = 2.85 keV, measured fwhm = 2.82 keV. For the calculation in (b), reverse geometry, detector o.d. = 4.2 cm, and  $\lambda_h = 500$  cm were used. Measured detector had o.d. = 4.2 cm, i.d. = 1.0 cm, depletion voltage = -900 V, operating bias = -2000 V and was exposed to  $5 \times 10^8$  n/cm<sup>2</sup>. Calculated fwhm was 2.08 keV and measured fwhm was 2.05 keV. For the calculation in (c) the parameters were the same as in (b) except  $\lambda_h = 140$  cm. Measured detector was the same as in (b) except the operating bias was reduced to -1000 V. Calculated fwhm was 2.42 keV and measured fwhm was 2.46 keV.

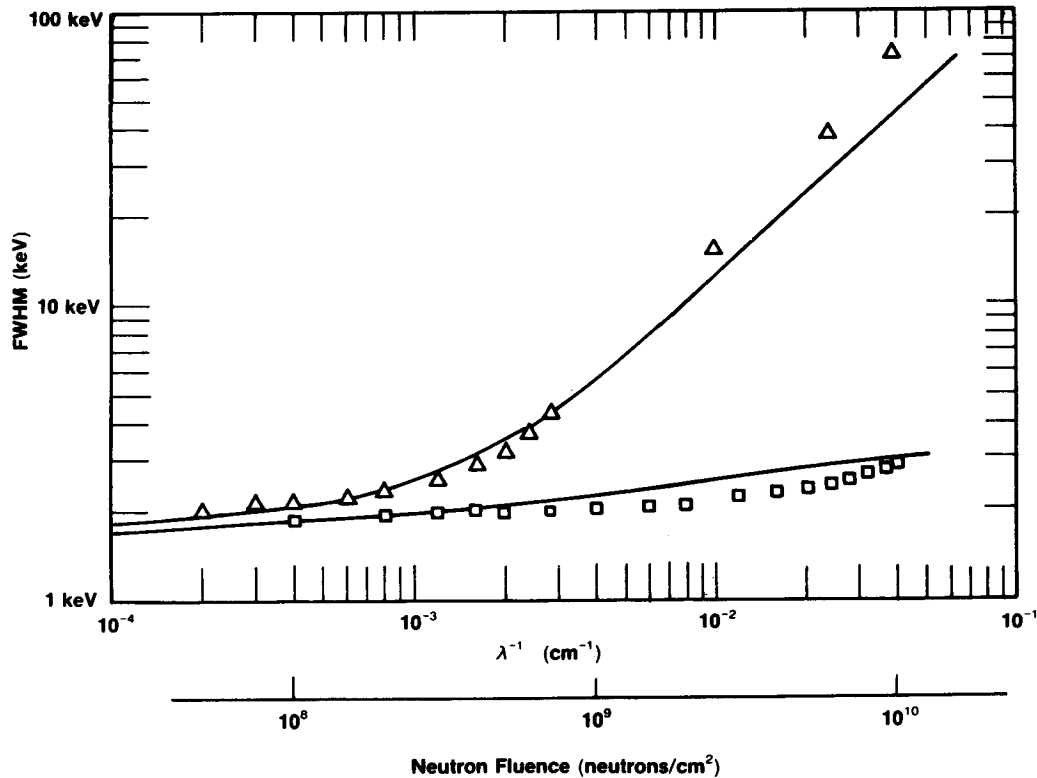


Fig. 2. Comparison of calculated fwhm measurements at 1332 keV to experimentally measured spectra [4] for conventional (triangles) and reverse (squares) geometry HPGe coaxial detectors at various fast neutron fluences.

pronounced for coaxial detectors of reverse electrode geometry than for those of conventional geometry. Likewise, in contrast to the case of conventional geometry, the variation of fwhm with  $\lambda_h$  is not very dependent on  $r_2$ . In summary, the theory predicts that large diameter detectors having conventional electrode geometry will show far more degradation than small diameter detectors after a given fast neutron exposure. By contrast, reverse electrode coaxial detectors will display far less energy resolution sensitivity to the outer diameter after fast neutron exposure.

### 3.3. Line shape dependence on detector bias

The variation of line shape with detector bias may be inferred from the electric field dependence of  $\lambda_h$ . The electric field itself is a function of both  $r$  and applied bias,  $V$ , hence the mean free drift length,  $\lambda_h$ , is also a function of  $r$  and  $V$  by eqs. (19)–(23). As shown previously, when  $\lambda_h$  is a function of  $r$  and  $V$ , the calculation of  $\eta(r)$  requires the solution of equations such as eq. (24). Consequently, the exact evaluation of eq. (1) requires that three nested numerical integrations be performed. Such a procedure would be unacceptably

slow on most desk-top computers since at least 5-figure accuracy is required for the determination of  $\eta(r)$ . As an approximation, the value of  $\lambda_h$  calculated from eq. (19) was directly substituted into eq. (8) and  $\eta(r)$  was evaluated as before. The energy resolutions calculated from line shapes determined by this procedure differed by no more than 10% from energy resolutions calculated from the few line shape curves generated by actually performing the triple numerical integrations. The approximation appears to be very good and was hence used in the following line shape determinations.

Figs. 5a and b illustrate the change in calculated line shape as a function of bias for detectors of conventional and reverse geometry, respectively, when  $v_{\text{drift}}$  and  $\langle v \rangle$  were allowed to vary with electric field according to eqs. (20) and (21). The product  $n_t \sigma_h$  was chosen so that the corresponding  $\lambda_h$  value at high electric field would result in a significantly asymmetric line shape for both detector geometries and was held constant in order to ascertain the effect of varying the  $v_{\text{drift}}/\langle v \rangle$  term alone. The parameter values used for the calculation are given in the caption. It may be seen from fig. 5 that large variations in the applied voltage, and hence the electric field and carrier velocities, do not result in large changes

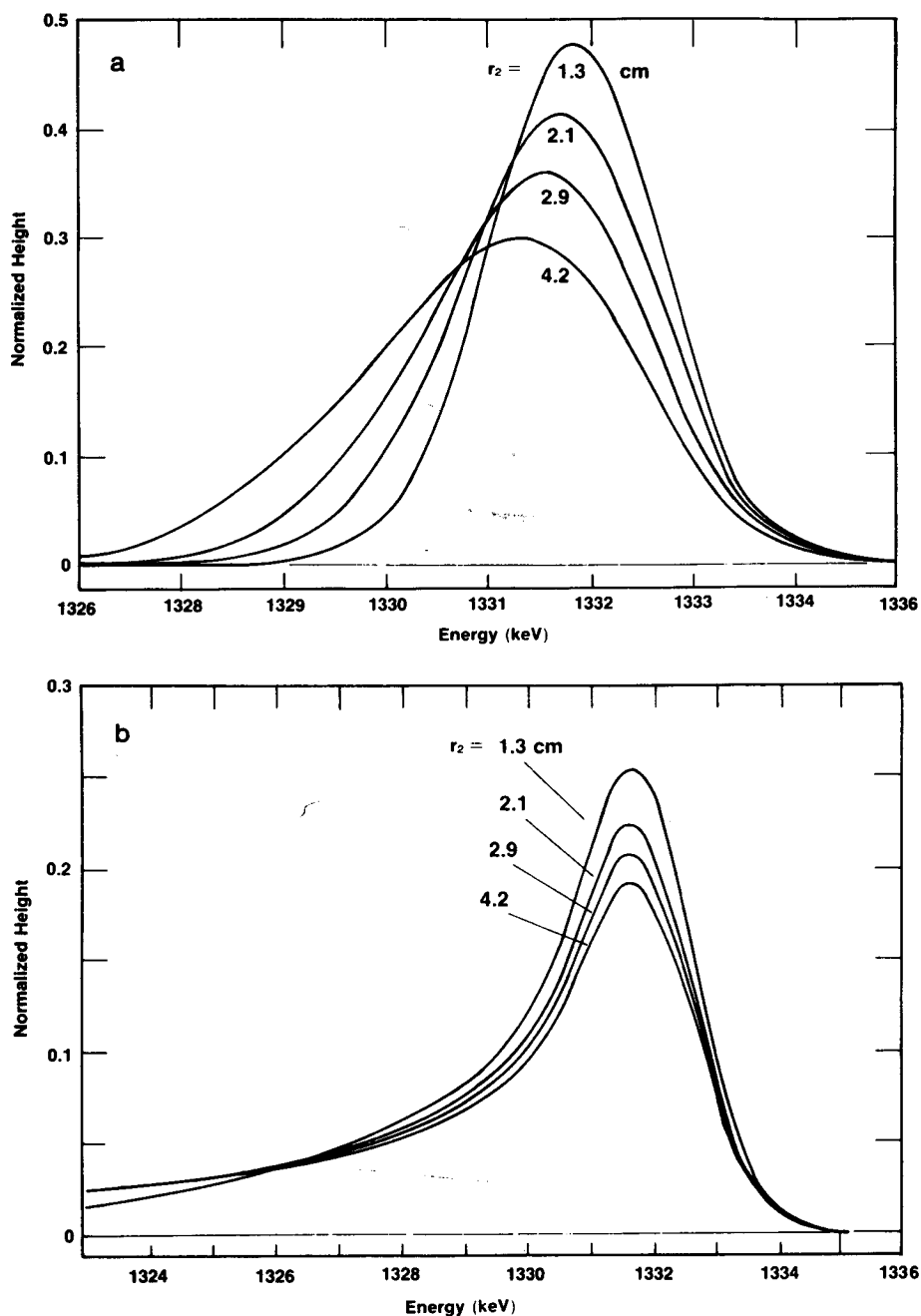


Fig. 3. Calculated effect of outer radius on line shape at 1332 keV for HPGe coaxial detectors with (a) conventional and (b) reverse geometry. Parameters of calculation: (a)  $\lambda_h = 1600$  cm, (b)  $\lambda_h = 50$  cm. For (a) and (b)  $\lambda_e = 10^7$  cm, inner radius = 0.5 cm, outer radius as noted on curves, electronic noise = 550 eV,  $K = 340$  and  $F = 0.12$ .

in line shape. In fact, very small values of the charge density  $\rho$ , corresponding to low depletion voltages, had to be used in the calculation in order to generate electric field values weak enough to produce reasonable differences in the line shapes shown in fig. 5. This

relative insensitivity to carrier velocity was previously noted by Sher [3].

Large changes in fwhm and peak position are, however, observed as the electric field varies. To account for these observations it is necessary to assume that the

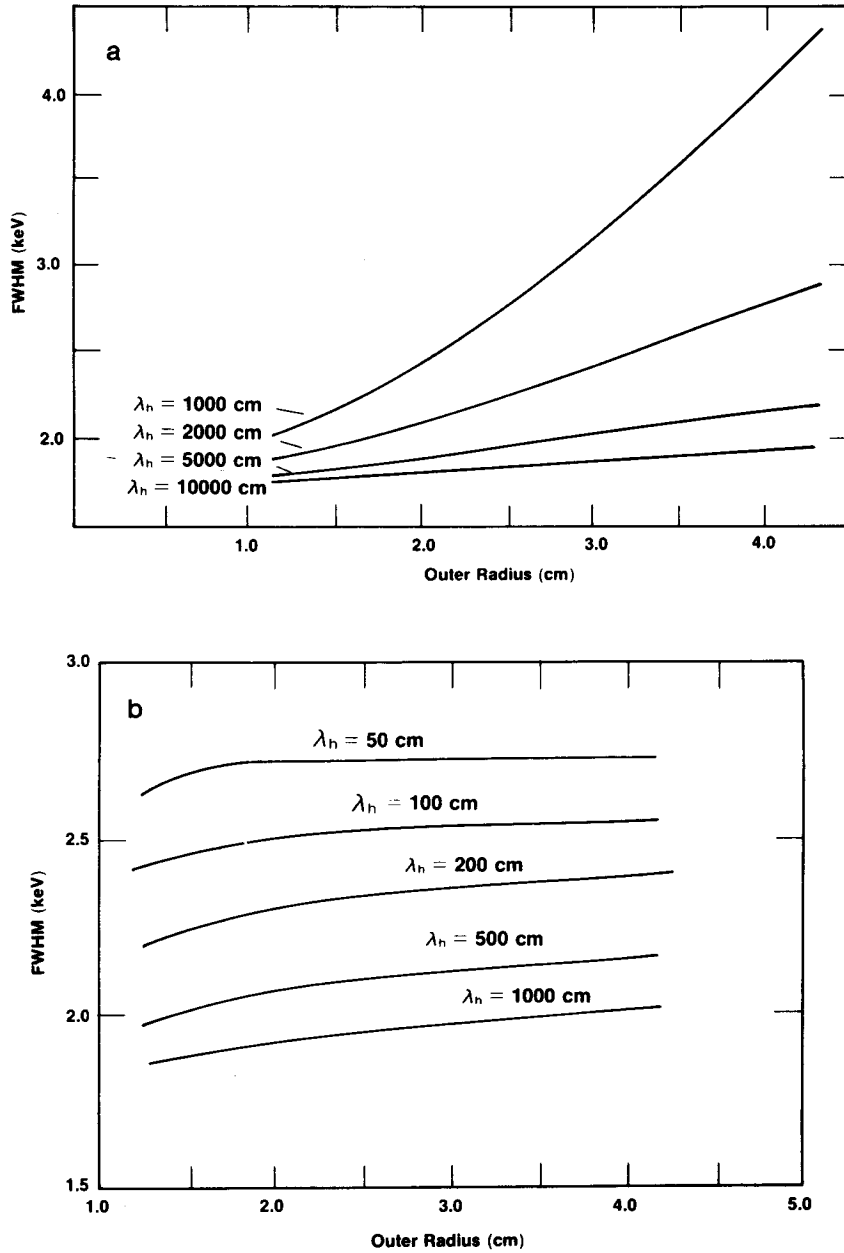


Fig. 4. Calculated effect on fwhm when detector radius is varied for HPGe coaxial detectors with (a) conventional and (b) reverse geometry.  $\lambda_h$  treated as a parameter of the calculation. Other quantities are the same as for fig. 3.

effective carrier trap cross section is also a function of electric field. As mentioned previously, Darken et al. [15] proposed that the trap cross section of disordered regions created in germanium by fast neutrons is proportional to  $\mathcal{E}^{-1}$ . Therefore, a line shape calculation which includes the field dependence of  $\sigma_h$  may be performed by substituting eq. (23) with  $x = 1$  into eq. (19).  $\mathcal{E}$  is again given by eq. (22) and  $v_{drift}/\langle v \rangle$  allowed

to vary with field as before. The parameters left to be determined are the proportionality constant,  $\sigma_0$ , in the expression for  $\sigma_h$ , and the trap density,  $n_t$ .

Since the mean free path of fast neutrons in Ge is approximately 6 cm, an average value for  $n_t$  of between  $5$  and  $6 \times 10^7/\text{cm}^3$  results when a detector 6 cm in length is exposed to  $5 \times 10^8$  fast neutrons/ $\text{cm}^2$ . Fast neutron fluences in the  $10^8$ – $10^9$  neutrons/ $\text{cm}^2$  range

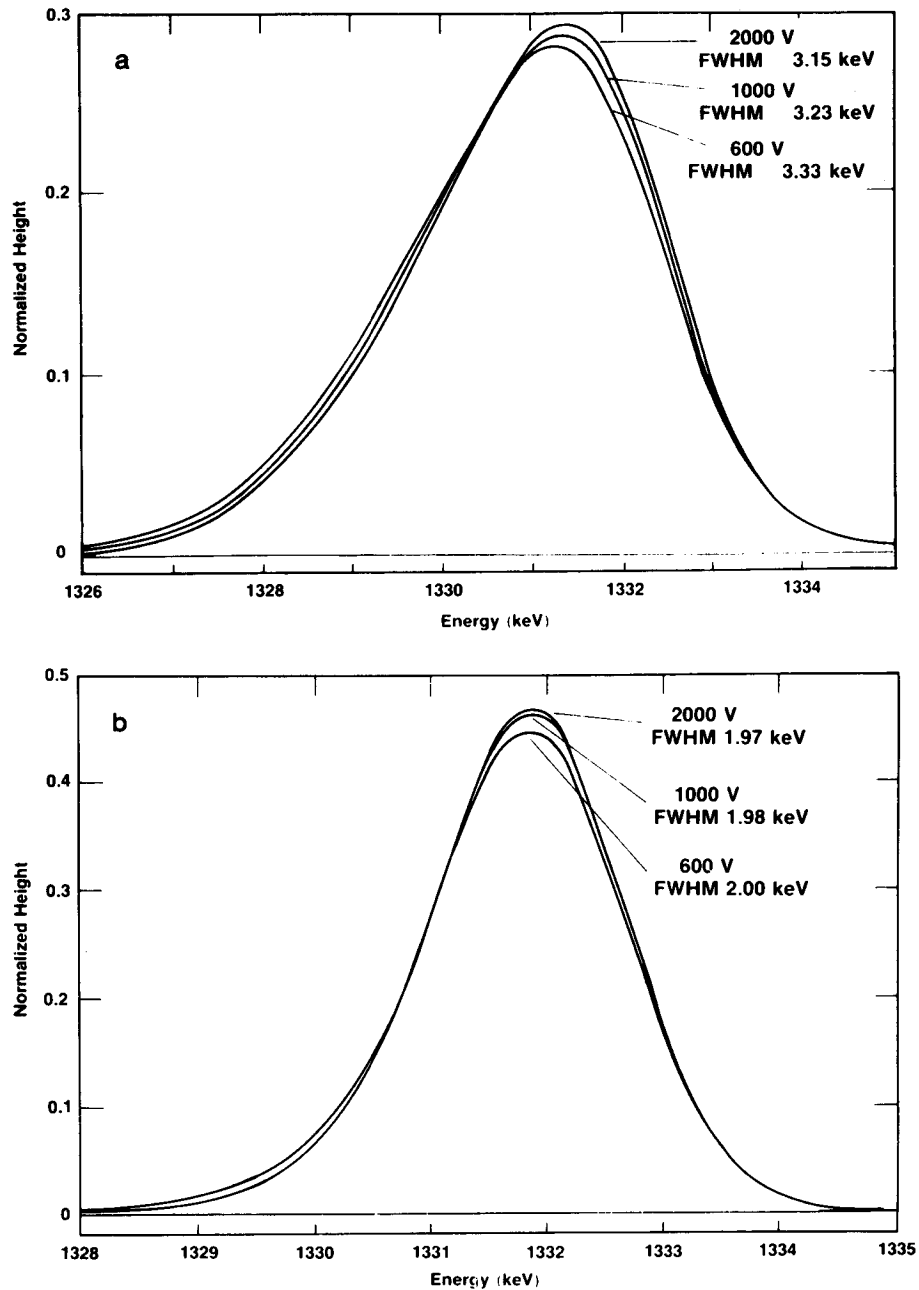


Fig. 5. Calculated effect at 1332 keV of the variation in carrier velocity on line shape for coaxial detectors having (a) conventional and (b) reverse geometry. Parameters of the calculation for (a) and (b):  $K = 340$ ,  $F = 0.12$ , electronic noise = 550 eV,  $\lambda_e = 10^7$  cm, detector o.d. = 5.8 cm, detector i.d. = 1.0 cm, depletion voltage = 500 V and  $n_t \sigma_h = 5 \times 10^{-4}/\text{cm}$ .

generally cause significant damage in conventional geometry but relatively negligible damage in reverse geometry coaxial detectors, as demonstrated in fig. 2. Darken et al. [14] estimated a trap cross section of  $\sim 10^{-11} \text{ cm}^2$  for the particular reverse electrode detector under investigation. Since most of the volume of this device was subject to electric fields of  $\mathcal{E} \geq 2000 \text{ V/cm}$ ,

for our calculation we chose  $\sigma_0$  such that, at an electric field of 2000 V/cm,  $\sigma_h = 10^{-11} \text{ cm}^2$ . Thus, from eq. (23),  $\sigma_0 = 2 \times 10^{-8} \text{ V cm}$ . In addition,  $n_t = 5.5 \times 10^7 \text{ cm}^{-3}$  was assumed in order to correspond to a fluence of  $5 \times 10^8 \text{ neutrons/cm}^2$ . Fig. 6 presents the bias dependence of the line shape for (a) conventional and (b) reverse geometry cases when the field dependence of  $\sigma_h$

and the carrier drift and thermal velocities are taken into account.

It would be interesting to compare these curves to experimental spectra. Unfortunately, complete experimental line shape curves are not available. However, some previous measurements at various detector biases

were made in our laboratory of the fwhm, fwtm (full width at tenth maximum) and fwfm (full width at fiftieth maximum) of spectral lines originating from neutron-damaged detectors. Table 1 shows the component of the fwhm, fwtm and fwfm due to trapping as determined by subtracting in quadrature the system

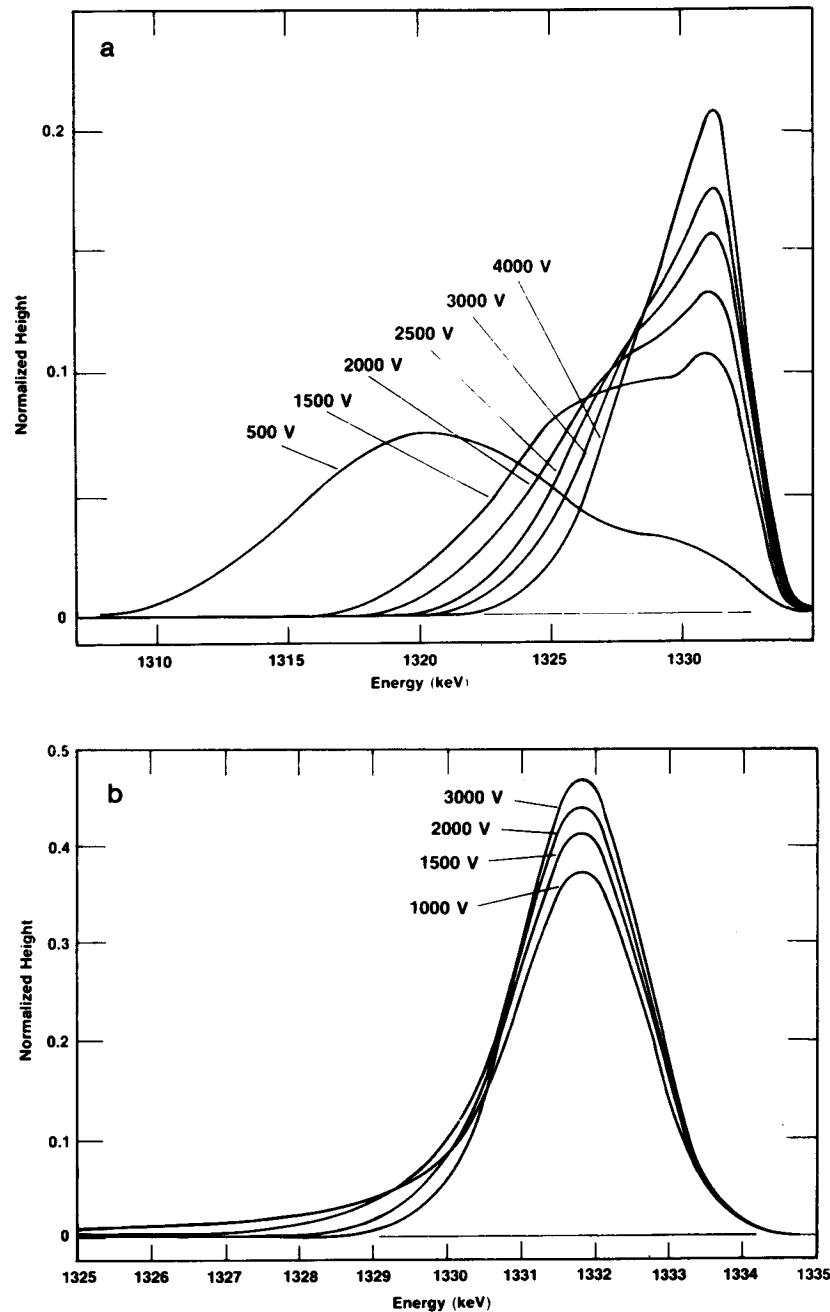


Fig. 6. Calculated effect of the variation in both the carrier velocity and the trap cross section with bias voltage for coaxial detectors having (a) conventional geometry and (b) reverse geometry. Parameters of the calculation:  $n_i = 5.5 \times 10^7/\text{cm}^3$ ,  $\sigma_h = 2 \times 10^{-8}/\text{cm}^2$ , other quantities as in fig. 1.

Table 1

Calculated component of the energy resolution due to trapping vs measured trapping component values for a detector having conventional geometry

| Bias [V] | Calculation |            |            | Measurement |            |            |
|----------|-------------|------------|------------|-------------|------------|------------|
|          | fwhm [keV]  | fwtm [keV] | fwfm [keV] | fwhm [keV]  | fwtm [keV] | fwfm [keV] |
| 1500     | 9.47        | 14.34      | 17.42      | 9.12        | 15.42      | 20.35      |
| 2000     | 7.48        | 12.16      | 15.26      | 7.28        | 13.31      | 18.81      |
| 2500     | 6.22        | 10.76      | 13.62      | 6.10        | 11.53      | 16.26      |
| 3000     | 5.32        | 9.74       | 12.51      | 5.48        | 10.22      | 14.84      |

noise and the zero-damage resolution from fig. 6a. These quantities are then compared to the values obtained from an actual neutron-damaged conventional geometry detector (o.d. 5.8 cm, i.d. 0.9 cm, length 5.8 cm and depletion voltage 400 V). This particular device had been exposed to a fluence of only  $1.1 \times 10^8$  n/cm<sup>2</sup> from an unmoderated Pu-Be source but was then warmed to room temperature for 48 h before being cooled again. Conventional geometry detectors always exhibit significant resolution degradation after such a warm period and, after the warm time, this detector demonstrated a spectrum roughly comparable to those of the line shapes shown in fig. 6a. The data from this device therefore proved useful for making the desired comparison. The measured neutron-damage trapping component of the fwhm at 3000 V is very close to the value calculated from fig. 6a and the agreement between the calculated and measured values at lower biases is excellent. This agreement between measured and calculated voltage dependences strongly supports the hypothesis that the trap cross section is proportional to  $\mathcal{E}^{-1}$ . One should also note that the warm period dramatically increases the resolution degradation. The calculation was performed for a trap density of  $5.5 \times 10^7$ /cm<sup>3</sup>, corresponding to a fluence of approximately  $5 \times 10^8$  neutrons/cm<sup>2</sup>. The detector had actually only received  $1.1 \times 10^8$  neutrons/cm<sup>2</sup>, at which point its performance had just slightly degraded (fwhm = 2.07 keV). However, the 48-h warm period caused its spectrum to be comparable to the spectrum calculated for a five-times greater neutron fluence. According to the calculation, therefore, the 48-h warm time was equiv-

alent in effect to a five-fold increase in fast neutron exposure.

Table 2 presents the component of the fwhm, fwtm and fwfm due to trapping as calculated from the curves of fig. 6b, and also shows the measured values obtained from a neutron-damaged detector (o.d. 4.2 cm, i.d. 1.0 cm, length 4.1 cm, depletion voltage 900 V) of reverse geometry. The detector had been exposed to a fluence of  $5 \times 10^8$  n/cm<sup>2</sup> from an unmoderated Pu-Be source, which was the same fluence assumed for the calculation. The correspondence between calculated and measured values is very good. In particular, the calculation reproduces the slow variation of the fwhm and the large variation of the fwfm with detector bias. The correlation between calculated and measured quantities indicates that the numerical values chosen for parameters  $n_t$  and  $\sigma_0$  were fairly accurate estimates and gives further support to the neutron-damage model of Darken et al. [15].

Theoretical curves in which  $\sigma_h$  was varied using different electric field dependences were also calculated. Fig. 7 shows three such curves generated using the same detector parameters as for fig. 6a at a bias of 1500 V. The curves labeled 0.9 and 1.1 denote electric field dependences of  $\mathcal{E}^{-0.9}$  and  $\mathcal{E}^{-1.1}$ , respectively, while that labeled 1.0 is the same 1500 V line shape shown in fig. 6a. The fwhm of 9.47 keV determined for the curve marked 1.0 is very close to the measured value of 9.12 keV shown in table 1 whereas the other two obviously are not. Furthermore, the  $\mathcal{E}^{-0.9}$  and  $\mathcal{E}^{-1.1}$  field dependences result in bias dependent energy resolutions that are quite different from the measured values listed in table 1. These results strongly indicate that the trap

Table 2

Calculated component of the energy resolution due to trapping vs measured trapping component values for a detector having reverse geometry

| Bias [V] | Calculation |            |            | Measurement |            |            |
|----------|-------------|------------|------------|-------------|------------|------------|
|          | fwhm [keV]  | fwtm [keV] | fwfm [keV] | fwhm [keV]  | fwtm [keV] | fwfm [keV] |
| -1000    | 1.20        | 3.40       | 8.79       | 1.31        | 4.50       | 9.47       |
| -1500    | 1.15        | 3.26       | 5.35       | 1.21        | 3.14       | 5.13       |
| -2000    | 1.10        | 2.69       | 4.14       | 1.00        | 2.48       | 3.90       |
| -3000    | 0.96        | 2.04       | 2.94       | 0.79        | 1.63       | 2.28       |

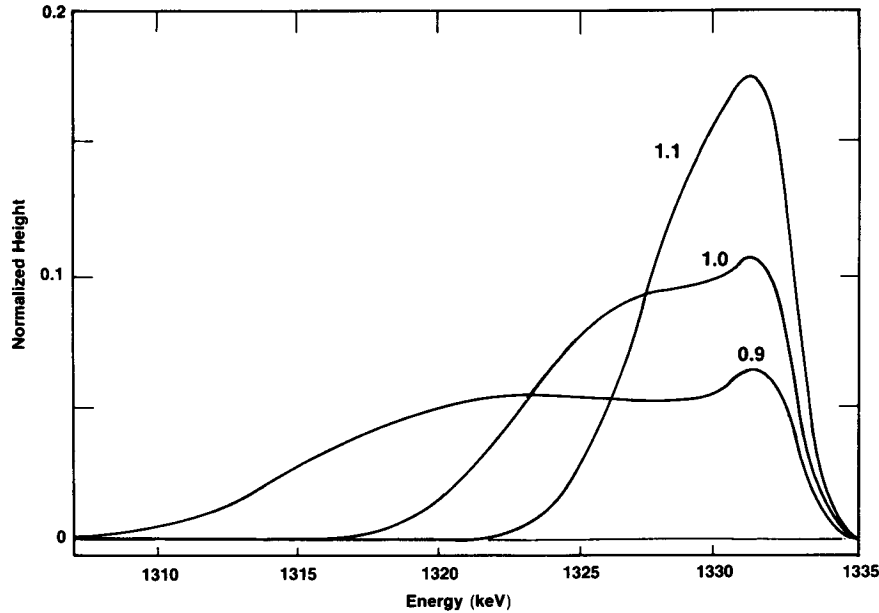


Fig. 7. Calculated line shape curves for different electric field dependences of  $\sigma_h$  for a coaxial detector having conventional geometry. Curves labeled 0.9, 1.0 and 1.1 represent electric field variations of  $\sigma_h$  proportional to  $\mathcal{E}^{-0.9}$ ,  $\mathcal{E}^{-1.0}$ ,  $\mathcal{E}^{-1.1}$ , respectively, at a bias of 1500 V. Other parameters are the same as for fig. 6a.

cross section for fast neutron induced trapping in HPGe detectors indeed has an electric field dependence represented by  $\sigma_h \propto \mathcal{E}^{-1.0}$ .

#### 4. Summary and conclusions

The purpose of this work was to develop a theoretical method to predict and quantify the effects of charge carrier trapping on HPGe coaxial detector line shapes. A model was developed based on the Trammell-Walter equation. In this model, the term for the standard deviation of pulse height ( $\sigma_T$ ) was given a positional dependence which differed appreciably from relationships proposed by previous authors. As distinct from earlier attempts to mathematically generate line shapes, collimated beam measurements on the particular detector under investigation were not necessary to determine any parameter of the calculation.

The model was then used to calculate line shapes which closely matched the measured line shapes of both conventional and reverse electrode HPGe coaxial detectors that had suffered fast neutron damage. The relative resistance to the effects of fast neutron irradiation of detectors having the two different electrode configurations was calculated and found to be very similar to experimentally established behavior. Fig. 2 illustrates this excellent correlation. Since this damage is uniformly distributed, the calculated gamma-ray line shapes

are not dependent on whether the charge is generated by single or multiple interaction events if the assumption of uniform gamma-ray irradiation is satisfied\*. The theory also predicts the energy resolution and line shape of neutron-damaged conventional geometry HPGe coaxial detectors to be very dependent on detector diameter. On the other hand, the performance of neutron-damaged HPGe coaxial detectors with reverse geometry was predicted to show much less dependence on the diameter. The calculations also demonstrate that the drift velocity variations of the carriers have a minimal effect on the fwhm and line shape of neutron damaged HPGe coaxial detectors of either contact geometry, at least over a realistic range of electric fields. The theory also reveals that the generally observed variation of the energy resolution and line shape as a function of bias voltage mainly arises from the dependence of the trap cross section on electric field. Neutron-damaged conventional electrode geometry HPGe coaxial detectors are predicted to exhibit a larger variation of the line shape with field than similarly damaged reverse electrode detectors. The correspondence of the calculated effects to measured values is extremely good when the trap cross section,  $\sigma_h$ , is assumed to vary as  $\mathcal{E}^{-1}$ .

The success of this model in predicting the effect of

\* The assumption of uniform gamma-ray irradiation is not satisfied for low energy photons entering from the side of a coaxial detector or from the face of a planar detector.

fast neutron irradiation on detector line shapes could provide a means of measuring fast neutron fluences on the basis of detector performance. By adjusting the parameter  $n_t$  so that a calculated line shape fits a measured spectrum, an estimate of the fast neutron fluence may be made. In this regard, a HPGe coaxial detector of conventional geometry might be employed as a sensitive (but expensive) fast neutron detector for low fluences, especially if use is made of the damage enhancement effect of thermal cycling.

The theory developed here is quite general and the actual cause of trapping is not a parameter of the calculation. As long as the trap density and trap cross sections are known, any source of trapping may be analyzed. In fact, the trap density or cross section (but not both simultaneously) may be estimated by considering them fitting parameters for line shape calculations. Characterization of HPGe crystals by analysis of the detector line shape could also be accomplished if an appropriate expression for the often nonuniform trap distribution,  $n_t$ , were used.

#### Acknowledgements

We would like to thank M. Martini for providing the encouragement necessary for us to start this project. We would also like to thank F. Goulding and R. Trammell along with M. Martini for some extremely useful and helpful discussions. In addition we are grateful to P. Pehl for her expert editorial assistance. Much apprecia-

tion is also due A. Moore for typing the manuscript in its many versions.

#### References

- [1] R. Trammell and F.J. Walter, Nucl. Instr. and Meth. 76 (1969) 317.
- [2] T.A. McMath and M. Martini, Nucl. Instr. and Meth. 86 (1970) 245.
- [3] A.H. Sher, IEEE Trans. Nucl. Sci. NS-18 (1971) 175.
- [4] R.H. Pehl, N.W. Madden, J.H. Elliott, T.W. Raudorf, R.C. Trammell and L.S. Darken Jr., IEEE Trans. Nucl. Sci. NS-16 (1979) 321.
- [5] H.W. Kraner, C. Chasman and K.W. Jones, Nucl. Instr. and Meth. 62 (1968) 173.
- [6] T.W. Raudorf, M.O. Bedwell and T.J. Paulus, IEEE Trans. Nucl. Sci. NS-29 (1982) 764.
- [7] Z.H. Cho and J. Llacer, Nucl. Instr. and Meth. 98 (1972) 461.
- [8] R.C. Trammell, M.S. Thesis, Univ. of Tennessee (1969).
- [9] H.R. Bilger, Phys. Rev. 163 (1967) 163.
- [10] R. Henck, D. Gutknecht, P. Siffert, L. DeLaet and W. Schoenmackers, IEEE Trans. Nucl. Sci. NS-17 (1970) 149.
- [11] T.W. Raudorf, R.C. Trammell, S. Wagner and R.H. Pehl, IEEE Trans. Nucl. Sci. NS-31 (1984) 253.
- [12] C. Canali, G. Majni, R. Mindes and G. Ottaviani, IEEE Trans. Elec. Dev. (Nov. 1975) 1045.
- [13] W.E. Pinson and R. Bray, Phys. Rev. A136 (1964) 1449.
- [14] L.S. Darken Jr., R.C. Trammell, T.W. Raudorf and R.H. Pehl, IEEE Trans. Nucl. Sci. NS-28 (1981) 572.
- [15] L.S. Darken Jr., R.C. Trammell, T.W. Raudorf, R.H. Pehl, and J.H. Elliott, Nucl. Instr. and Meth. 171 (1980) 49.